Morphology Effect on the UV Photodetection Properties of Li-doped ZnO Nanorods Array

Yu-Mau Hong
Department of Electrical Engineering
Hsiuping University of Science and Technology, Taichung 41280, Taiwan

San-Lin Young*
Department of Electronic Engineering
Hsiuping University of Science and Technology, Taichung 41280, Taiwan

Meng-Fen Ho
Department of Electronic Engineering
Hsiuping University of Science and Technology, Taichung 41280, Taiwan

Sung-Te Chen
Department of Electronics Engineering
Hsiuping University of Science and Technology, Taichung 41280, Taiwan

Abstract- The $Zn_{0.99}Li_{0.01}O$ nanorod arrays have been grown on the ZnO seeded p-type Si substrates with various growth time for nanostructural and optical properties investigation and for UV photodetection observation. Four different growth time of the $Zn_{0.99}Li_{0.01}O$ nanorod arrays were fabricated by the hydrothermal technique with growth time 15, 30, 45 and 60 minutes, respectively. The FE-SEM images show that the length of the nanorod arrays increases obviously with increasing growth time, while the diameter increase mildly. The x-ray diffraction patterns reveal that all nanorod arrays exhibit the same wurtzite structure with a preferential orientation along the c-axis. Besides, the photoluminescence spectra of all nanorod arrays show the same ultraviolet emission indicating the similar crystallite state with an optical bandgap of 3.28 eV and no obvious difference indicating the same oxygen defects in all $Zn_{0.99}Li_{0.01}O$ nanorod arrays. Finally, the I-V curves are separately measured in the dark and under UV illumination. The results show an increase of current variation ratio defined as $(I_{photo}-I_{dark})/I_{dark}$ with increasing $Zn_{0.99}Li_{0.01}O$ nanorod arrays indicating an enhancement of ultraviolet photodetection characteristics which may be resulted from the increase of surface area due to the increase of nanorod length.

Keywords – Zinc oxide, nanorod, seed layer, UV photodetection characteristics.

I. INTRODUCTION

Solid-state photodetectors based on compound semiconductors other than silicon opens new possibilities for commercial applications [1-2]. Compared with Si-based devices, ultraviolet (UV) photodetectors with wide bandgap semiconductors are especially attractive due to solar-blind ultraviolet detection property [3]. The compound semiconductor ZnO with a wide bandgap of 3.37 eV, high thermal stability, low-cost synthesis processes and compatibility with Si-based microelectronics makes itself become one of the most promising photonic materials for UV photodetection [4]. Recent researches further denoted that synthesis, characterization, and novel applications of the one-dimensional ZnO nanostructures have been intensive subjects due to their remarkable electrical, optical, and chemical properties [5]. Numerous researches have been reported on the ZnO-based UV detectors with one-dimensional nanostructures for the improvement of photonic characteristics [6]. Although ZnO-based one-dimensional nanostructures have been fabricated through various methods, the hydrothermal method offers more merits due to easier control of chemical composition and more simple method with a low-cost manufacturing process compared with other high vacuum fabrication processes [7]. For the application of ZnO-based semiconductors on electronic devices, the conventional method to produce *p*-type semiconductors is to dope elements with the group III or transitional metals in the ZnO-based compounds [8-9]. The *p*-type doped ZnO is

known to be easily synthesized. However, the fabrication of the *p*-type ZnO-based optoelectronic devices has met the challenges of both low reproducibility and the lack of low-resistivity [10]. The *p*-type ZnO can be achieved by the doping of group I elements. In this study, the smaller element Li of the group I, compared with Zn, is designed to dope into the ZnO nanorods and four different growth time are designed to grow $Zn_{0.99}Li_{0.01}O$ nanorods for the investigation of the nanostructural and optical properties. Besides, the application of the $Zn_{0.99}Li_{0.01}O$ nanorod arrays on the ZnO seeded *p*-Si substrates for UV photodetection is also discussed.

II. EXPERIMENTAL

The $Zn_{0.99}Li_{0.01}O$ nanorod arrays were fabricated by the hydrothermal method on ZnO seeded *p*-Si substrates with the growth time 15, 30, 45 and 60 minutes, respectively. The substrates were ultrasonically cleaned in the acetone, ethanol, and deionized (DI) water each for 10 min successively. The *p*-Si substrates with 0.55 Ω·cm resistivity were also ultrasonically cleaned in the acetone, ethanol, and deionized (DI) water each for 10 min successively and further wet etching step in HF (10%) solution was followed for 5 min to remove the native silicon oxide. Then, the *p*-Si substrates were rinsed in DI water and dried in flowing nitrogen gas. After the substrate cleaning processes, the sol-gel spin-coating ZnO seed layers were deposited on the *p*-Si substrates. The $Zn_{0.99}Li_{0.01}O$ nanorod arrays were grown on the ZnO-seeded *p*-Si substrates separately by the low-temperature hydrothermal method. The source solutions for $Zn_{0.99}Li_{0.01}O$ nanorod arrays growth were prepared with the precursors, including zinc acetate dehydrate $Zn(C_2H_3O_2)_2{\cdot}2H_2O$, lithium acetate dehydrate $LiCH_3COO{\cdot}2H_2O$ and hexamethylenetetramine $(CH_2)_6N_4$, in stoichiometric proportion dissolving in the DI water. Then, the ZnO-seeded *p*-Si substrates were placed upside down into the solution contained in closed vials at 90°C for 15, 30, 45 and 60 minutes, respectively, to grow the $Zn_{0.99}Li_{0.01}O$ nanorod arrays. Finally, the indium solder balls were pressed on the top of both the $Zn_{1-x}Li_xO$ nanorod arrays and the *p*-Si substrates to the measure the I-V curves.

The crystal structure of both $Zn_{0.99}Li_{0.01}O$ nanorod arrays was determined by the x-ray diffraction (XRD) patterns using a Rigaku D/max 2200 x-ray diffractometer with Cu-Kα radiation. The XRD data were recorded in the 2θ range from 20° to 60° with a step width of 0.01° and a scan speed of 0.5°/min. The surface morphologies and cross-section images of the nanorods were observed by a field emission scanning electron microscope (FE-SEM, JEOL JSM-6700F) at 3.0 kV. Then, photoluminescence (PL) spectrometer was used to measure the optical emissions of all $Zn_{0.99}Li_{0.01}O$ nanorod arrays from 330 to 645 nm by a 325 nm He-Cd laser. Finally, the current-voltage (I-V) curves of both $Zn_{0.99}Li_{0.01}O$ nanorod arrays with the bias voltage from -5 V to 5 V were performed in the dark and under UV illumination using the two-point probe I-V curve method with a Keithley 2400 source meter.

III. RESULTS AND DISCUSSION

Figure 1 shows the FE-SEM images with tiling 45° angle of the $Zn_{0.99}Li_{0.01}O$ nanorod arrays grown on the ZnO seeded *p*-type Si substrate with growth time 15, 30, 45 and 60 minutes, respectively. The length and diameter of the nanorods increases with increasing the growth time. The result indicates the length and diameter of the $Zn_{0.99}Li_{0.01}O$ nanorods may be controlled by the growth time with the hydrothermal method.

Figure 2 shows the XRD patterns of the $Zn_{0.99}Li_{0.01}O$ nanorod arrays. As the XRD patterns shown, the $Zn_{0.99}Li_{0.01}O$ nanorod arrays are found to have the same wurtzite hexagonal structure with space group P63/mc. Except for the Si substrate peak, the higher peaks intensity of the ZnO nanorod arrays with a longer grow time of the $Zn_{0.99}Li_{0.01}O$ nanorod arrays indicates the growth of $Zn_{0.99}Li_{0.01}O$ crystal which is the corresponding increase of nanorods length. The result is consistent with the results observed from the FE-SEM images.

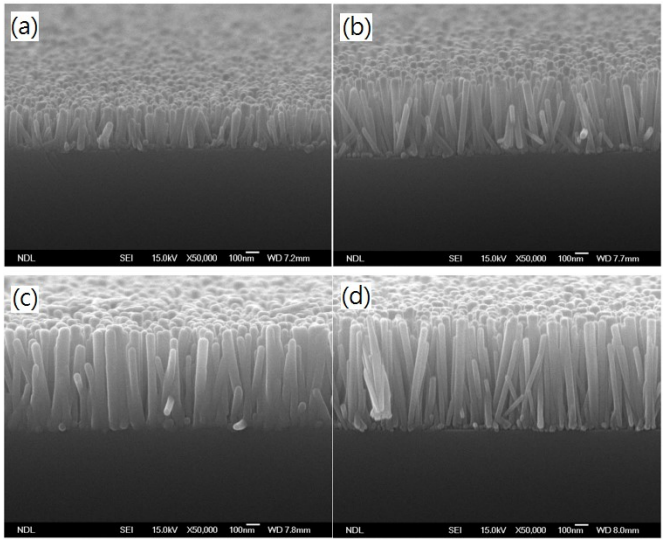

Figure 1. FE-SEM top-view images with tiling 45° angle of the $Zn_{0.99}Li_{0.01}O$ nanorod arrays grown on the ZnO seeded *p*-type Si substrate with growth time 15, 30, 45 and 60 minutes.

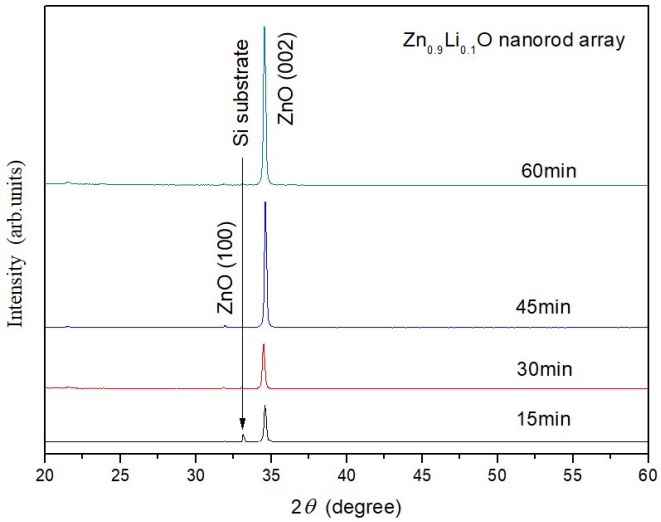

Figure 2. XRD patterns of the $Zn_{0.99}Li_{0.01}O$ nanorod arrays grown on the ZnO seeded *p*-type Si substrate with growth time 15, 30, 45 and 60 minutes.

Figure 3(a) shows the PL spectra and Figure 3(b) normalized PL spectra of all $Zn_{0.99}Li_{0.01}O$ nanorod arrays grown on the ZnO seeded *p*-type Si substrate with growth time 15, 30, 45 and 60 minutes, respectively. As shown in the Fig. 3(a), there is a strong emission peak at about 377.6 nm in UV band and a weak broad-band emission peak at 570 nm in the visible band. The UV emission peak is originated from excitonic recombination corresponding to the near-band-edge emission and the green emission is attributed to the recombination of electrons trapped in single ionized oxygen vacancies with holes [11]. In particular, the PL spectra of all $Zn_{0.99}Li_{0.01}O$ nanorod arrays grown on the sputtered ZnO seeded *p*-type Si substrate with growth time 15, 30, 45 and 60 minutes are almost overlap indicating the same crystallite state with an optical bandgap of 3.28 eV calculated by the formula, E_g=1240/λ. However, no obvious difference of visible emission at about 570 nm as shown in the Figure 3(b), indicating almost the same oxygen defects in all $Zn_{0.99}Li_{0.01}O$ nanorod arrays.

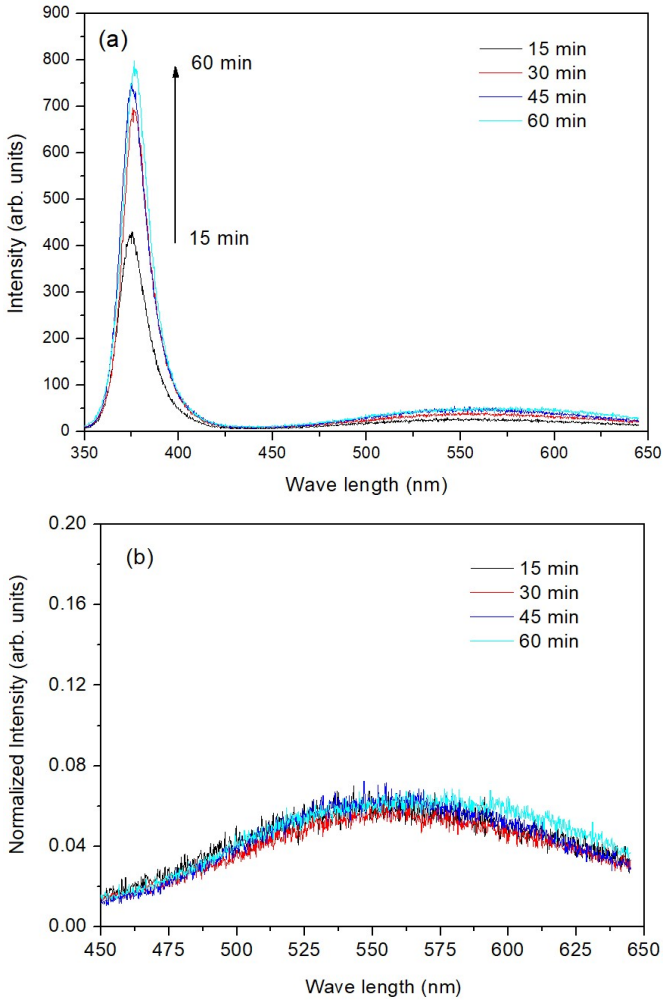

Figure 3. (a) Photoluminescence spectra of the $Zn_{0.99}Li_{0.01}O$ nanorod arrays grown on the ZnO seeded *p*-type Si substrate with growth time 15, 30, 45 and 60 minutes.

Figure 4 shows the I-V curves of all $Zn_{0.99}Li_{0.01}O$ nanorod arrays grown on the ZnO seeded *p*-type Si substrate with growth time 15, 30, 45, and 60 minutes, respectively. The I-V curves were measured both in the dark (dark-current, noted as I_{dark}) and under UV illumination (photo-current, noted as I_{photo}), respectively, for the exploration of the UV photodetection application. As listed in TABLE 1, the I_{dark} increases from 0.0328, 0.4608, 1.2528, to 1.3401 mA with the increase of $Zn_{0.99}Li_{0.01}O$ nanorod growth time from 15, 30, 45, to 60 minutes, due to the decrease of resistance resulted from the increase of diameter rather than length of the nanorods. The I_{photo} also increases obviously from 0.2706, 3.8749, 11.6009 to 12.6475 mA with the increase of nanorod time. Due to the obvious increase of nanorods length and diameter observed from the FE-SEM images as shown in Fig. 1 resulting in a largely increase of UV light-absorption surface area of the $Zn_{0.99}Li_{0.01}O$ nanorod arrays and the corresponding increase of UV light induced electron-hole pairs. The I_{dark} and I_{photo} current values measured at 5V along with UV photo-induced current variation ratio (R) of the $Zn_{0.99}Li_{0.01}O$ nanorod arrays in Table 1. The UV photo-induced current variation ratio R is defined as $(I_{dark}-I_{photo})/I_{dark}$ at 5V bias voltage to evaluate the UV photodetection characteristic. Due to the obviously increase of I_{photo} than I_{dark} with the nanorod growth time, the current variation ratio R increases apparently from 725%, 741%, 826%, to 844%. As a result, we obtain an increased UV photo-induced current variation ratio R with increasing $Zn_{0.99}Li_{0.01}O$ nanorod arrays growth time which illustrates the possibility for photodetection application.

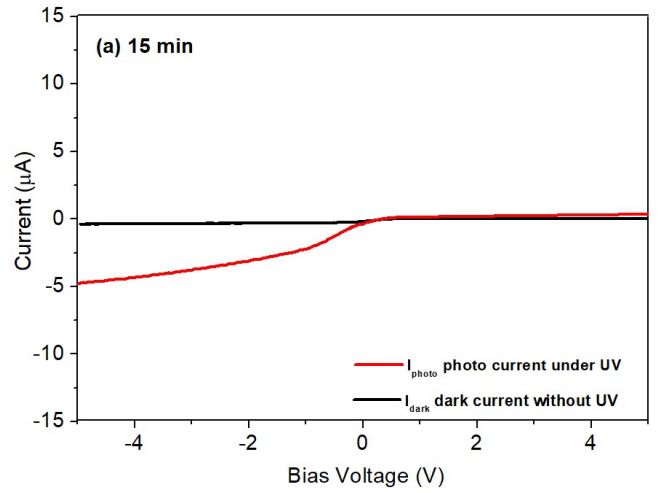
(a) 15 min
Current (μA)
Bias Voltage (V)
I photo photo current under UV
I dark dark current without UV

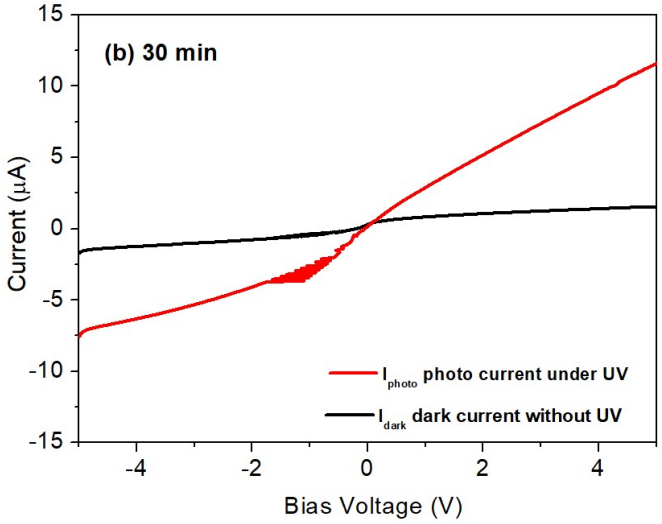
(b) 30 min
Current (μA)
Bias Voltage (V)
I photo photo current under UV
I dark dark current without UV

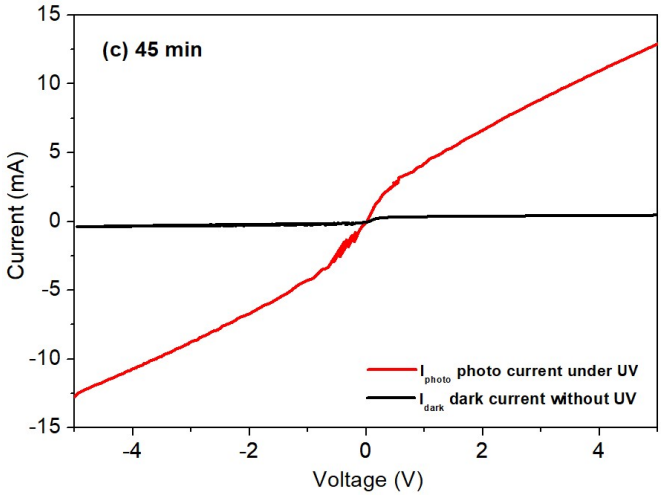
(c) 45 min
Current (mA)
Voltage (V)
I photo photo current under UV
I dark dark current without UV

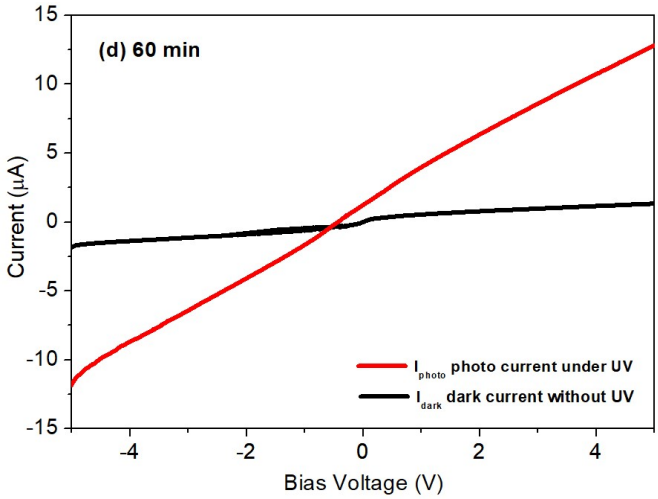

Figure 4. I-V curves in the dark and under UV illumination of the $Zn_{0.99}Li_{0.01}O$ nanorod arrays grown on the ZnO seeded *p*-type Si substrate with growth time (a) 15, (b) 30, (c) 45, and (d) 60 minutes.

TABLE 1. Dark and photo current values measured at 5V along with current variation ratio of of the $Zn_{0.99}Li_{0.01}O$ nanorod arrays grown on the ZnO seeded *p*-type Si substrate with growth time 15, 30, 45 and 60 minutes.

Sputtering time (minute)	**I_{dark} (μA)**	**I_{photo} (μA)**	**R (%)**
15	0.0328	0.2706	725%
30	0.4608	3.8749	741%
45	1.2528	11.6009	826%
60	1.3401	12.6475	844%

IV.CONCLUSION

The influence of nanorod growth time on the nanostructural, optical and electrical properties of the $Zn_{0.99}Li_{0.01}O$ nanorod arrays and corresponding application on the UV photodetection are investigated in this study. The morphology of the nanorods including length and diameter increase with increasing nanorod growth time. All XRD patterns of the $Zn_{0.99}Li_{0.01}O$ nanorod arrays reveal the same hexagonal wurtzite structure. PL spectra show the similar crystallite state with the same optical bandgap of 3.28 eV. From the I-V measured results, the UV photo-induced current variation ratio increase from 725% to 844% with the increase of grow time, which shows the possibility for UV photodetection application.

REFERENCES

[1] S. C. Dhanabalan, J. S. Ponraj, H. Zhang and Q. Bao, "Present perspectives of broadband photodetectors based on nanobelts, nanoribbons, nanosheets and the emerging 2D materials", *Nanoscale*, vol. 8, pp. 6410-6434, 2016.

[2] F. H. L. Koppens, T. Mueller, Ph. Avouris, A.C. Ferrari, M.S. Vitiello and M. Polini, "Photodetectors based on graphene, other two-dimensional materials and hybrid systems", *Nature Nanotechnology*, vol. 9, pp. 780-793, 2014.

[3] H. Chen, K. Liu, L. Hu, A. A. Al-Ghamdi and X. Fang, "New concept ultraviolet photodetectors", *Materials Today*, vol. 18, pp. 493-502, 2015.

[4] W. Tian, H. Lu, L. Li, "Photodetectors: materials, devices and applications", *Nano Research*, vol. 8, pp. 382-405, 2015.

[5] S. M. Ahmad and J. Zhu, "ZnO based advanced functional nanostructures: synthesis, properties and applications", Journal of Material Chemistry, vol. 21, pp. 599-614, 2011.

[6] C. -H. Chen and C. -T. Lee, "High detectivity mechanism of ZnO-based nanorod ultraviolet photodetectors", *IEEE Photonics Technology Letters*, vol. 25, pp. 348-351, 2013.

[7] S. -J. Young, C. -C. Yang and L. -T. Lai, "Review-growth of Al-, Ga-, and In-doped ZnO nanostructures via a low-temperature process and their application to field emission devices and ultraviolet photosensors", *Journal of The Electrochemical Society*, vol. 164, pp. B3013-B3028, 2017.

[8] S.H. Jeong, B.N. Park, S.-B. Lee and J.-H. Boo, "Study on the doping effect of Li-doped ZnO film", *Thin Solid Films*, vol. 516, pp. 5586-5589, 2008.

[9] J.G. Reynolds and C.L. Reynolds, "Progress in ZnO acceptor doping: What is the best strategy", *Advances in Condensed Matter Physics*, vol. 2014, pp. 457058-1-15, 2014.

[10] O. Maksimov, "Recent advances and novel approaches of p-type doping of ZnO", *Reviews on Advanced Materials Science*, vol. 24, pp. 26-34, 2010.

[11] C.C. Lin, S.L. Young, C.Y. Kung, H.Z. Chen, M.C. Kao, L. Horng, and Y.T. Shih, "Structural dependence of photoluminescence and room-temperature ferromagnetism in lightly Cu-doped ZnO nanorods", *IEEE Transaction on Magnetism*, vol. 47, pp. 3366-3368, 2011.